

Hydriding processes of Mg and Zr alloys by reactive milling

G. MULAS, L. SCHIFFINI, G. TANDA, G. COCCO*

Dipartimento di Chimica, Università di Sassari, Via Vienna 2, 07100 Sassari, Italy

E-mail: cocco@uniss.it

Mechanically alloyed Mg₂Ni/Ni nano-composite and Zr₅₅Cu₃₀Ni₅Al₁₀ amorphous powders were hydrogen charged at constant pressure under ball milling. While the Mg-based samples were able to absorb large amount of hydrogen under static conditions, and from the very onset of the mechanical treatment, an incubation milling period was needed for the hydrogen activation in the case of the amorphous sample. A progressively decreasing rate characterizes the process kinetics in the case of Mg₂Ni/Ni, whereas a self increasing sigmoid trend was observed for the multicomponent Zr alloy, which showed structural demixing phenomena in the absorption course. Irrespective of the system, the maximum absorption rate was strongly dependent on the milling intensity (Watt · g⁻¹). The hydriding rate (mole · g⁻¹s⁻¹) and the mechanochemical yield (mole · Joule⁻¹) were used to compare the processes on an absolute scale. In the case of Mg-based alloy, comparison was also made between mechanically induced and thermally (static) activated hydriding processes. Attempt was also made to work out the hydrogen atoms absorbed at the ball-hit event.

© 2004 Kluwer Academic Publishers

1. Introduction

It has been shown that structurally destabilized and nanocrystalline hydride systems can display better hydrogen storage capacity and enhanced ab- and desorption kinetics with respect to ordinary absorbing materials [1–4]. Mechanical alloying and grinding, mainly by ball milling, have been usually employed as processing techniques to refine the microstructure of the absorbing material to a nano scale. However, less work has been devoted to milling processes while hydriding, i.e., carried out under hydrogen atmosphere [5–8].

The aim of this contribution is to explore the milling conditions and process parameters that lead to possible improvement of the absorbing qualities under reactive milling and to find out possible correlations relating the absorbing kinetics to the dynamics of the mechanical treatment. We report on Mg- and Zr-based alloys characterized by different microstructures, highly strained, nanostructured and amorphous ones.

2. Experimental

The Mg₂Ni:Ni = 94:6 wt% nano-composite and Zr₅₅Cu₃₀Ni₅Al₁₀ amorphous alloy were prepared by ball milling starting from the pure elements. Metal powders at least of 99.9% purity from different sources were employed. Mechanical treatments were carried out in a commercial Spex Mod-8000 Mixer-Mill. As a reactor vial for the hydriding experiments we used specially

made hollow cylinders and covers. The cylinder was connected to the gas reservoirs (hydrogen, helium or argon) by means of a self-regulating valve, which ensures a constant working pressure inside the vial (0.4 MPa). The absorption kinetics was followed by monitoring the progressive pressure drop in the hydrogen reservoir. From it the hydriding rate was obtained in the usual mole · g⁻¹s⁻¹ unity.

The experimental methodologies developed to determine the milling parameters have been described in previous works [9, 10]. We showed that the kinetic energy pulse, E (J · hit⁻¹), released to the powder at each collision event and the collision frequency, N , (hit · s⁻¹), can be determined when the vial dynamics is known, milling experiments with a single grinding ball are carried out, and quasi-inelastic conditions are approached at the collision. Under these circumstances the dynamic features of the grinding motion are qualified by E and N . Together they define the specific milling intensity, I_M (Watt · g⁻¹), which represents the rate of mechanical energy transfer to the powder batch, m_p : $I_M = NE/m_p$. The total work done on the system in the time t is represented by the energy dose, D_M (Joule · g⁻¹), given by $D_M = I_M \cdot t$. The mechanochemical yield (mole · kJ⁻¹) is obtained by scaling the transformation rate to the I_M . The nomenclature first introduced by Butyagin has been followed [11].

The same collision frequency (29 hits · s⁻¹) and powder charge (about 8 g) were maintained constant, whereas the impact energy, and therefore the intensity

* Author to whom all correspondence should be addressed.

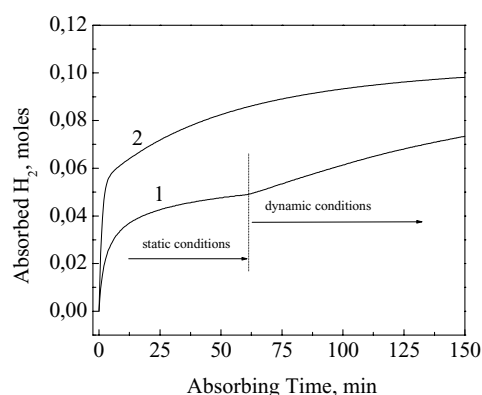


Figure 1 Absorbed hydrogen moles for Mg₂Ni/Ni powder samples as a function of the elapsed time. Curve 1 was collected under static absorbing conditions up to the marker, then under milling. Curve 2 refers to the process carried out under milling from the beginning. $I_M = 0.68 \text{ W} \cdot \text{g}^{-1}$.

was changed, by using balls of different masses. The working milling intensities are quoted in the text.

X-ray diffraction Analysis was used to characterize the microstructural features of the samples and the phase changes in the course of the treatment. Thermal and thermochemical properties were studied with DSC, TG, DTA and TPD techniques.

3. Results and discussion

We initially refer to Mg₂Ni/Ni system. Kinetic data shown in Fig. 1 refer to two parallel trials carried out under static conditions, i.e., simply pressurizing with H₂ the vial kept stationary (Curve 1), and under reactive milling conditions (Curve 2). Mechanical work produces a noticeable rise of the activated hydrogen molecules, even if, in both cases, the absorbing rate progressively decreases as a function of the elapsed time. The rising trend in curve 1 after about 60 min, marked by the dotted bar, is due to the action of the milling treatment, which was switched on with the static absorbing process going to saturation. The starting absorbing rate is calculated from the slope to the initial trend of Curve 1 and Curve 2, and is $3.6 \times 10^{-5} \text{ mole} \cdot \text{g}^{-1} \text{ s}^{-1}$, corresponding to $3.2 \times 10^{20} \text{ atoms} \cdot \text{s}^{-1}$, for the static absorbing conditions (Curve 1), and $8.2 \times 10^{-5} \text{ mole} \cdot \text{g}^{-1} \text{ s}^{-1}$, corresponding to $7.3 \times 10^{20} \text{ atoms} \cdot \text{s}^{-1}$, under reactive milling (Curve 2). The observed rate at

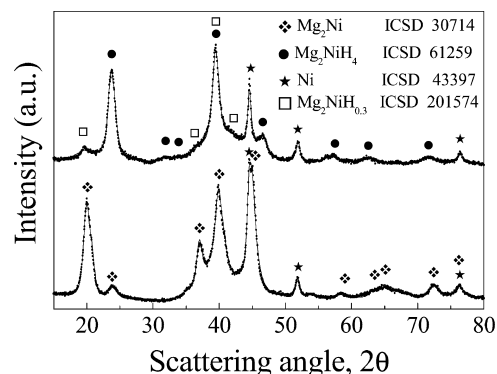


Figure 2 Cu K α XRD patterns of the Mg₂Ni/Ni as prepared powders (lower pattern), and at the end of the hydriding process carried by reactive milling (upper pattern). The phases quoted in the inset were assigned according to the Inorganic Crystal Structure Data Base.

the limit of the static absorption curve (dotted bar), $2.6 \times 10^{-7} \text{ mole} \cdot \text{g}^{-1} \text{ s}^{-1}$, increases to $4.4 \times 10^{-7} \text{ mole} \cdot \text{g}^{-1} \text{ s}^{-1}$ at the milling outset.

The XRD analysis according to fitting procedures and Rietveld methods [12] has allowed a complete characterization of the powder microstructure in the as prepared and fully hydrided powders. Some of the patterns are presented in Fig. 2. The reduced dimensions of the coherent scattering domains prove the nanostructured features of the as prepared samples. Ni patches are also present in the starting mixture 20 nm in size, from which a specific surface area of about $17 \text{ m}^2 \text{ g}^{-1}$ was evaluated according to well established procedures, as explained in the caption of Table I. Table I summarizes structural results and related quantities, including the phase percentage. The Mg₂NiH₄ phase is the major hydride phase in the final end products.

Let consider first the static or thermally activated absorbing process. An interconnected structure of incoherent interfaces and grain boundaries, forming an extended network of privileged high diffusivity paths for molecular hydrogen, can be surmised from either the structural analysis and the fast absorbing rate at the onset of the process. The Ni interphase seems therefore easy accessible to hydrogen, which, at the relatively high working pressure forms a complete and permanent multilayer coverage. Access to Ni surface is mandatory for the dissociative chemisorption of the hydrogen molecules, which is the preliminary step for

TABLE I Results of the XRD analysis

Phases	$\langle D \rangle^a$ (nm)	Strain (%)	Phase wt(%)	S_{sp}^b (m ² /g)	Surface atoms in the batch ^c	Surface atoms in $1 \times 10^{-4} \text{ g}^d$	Bulk atoms in the batch ^c	Bulk atoms in $1 \times 10^{-4} \text{ g}^d$
<i>As prepared</i>								
Mg ₂ Ni	6.0	6×10^{-3}	94.0	121.4	1.1×10^{22}	1.4×10^{17}	3.9×10^{22}	5.3×10^{17}
Ni	20.0	2×10^{-3}	6.0	16.9	1.2×10^{20}	1.6×10^{15}	4.6×10^{21}	6.2×10^{16}
<i>After Hydriding</i>								
Mg ₂ NiH _{0.3}	4.0	1×10^{-2}	39.5	182.2				
Mg ₂ NiH ₄	11.4	5×10^{-3}	54.0	145.4				
Ni	40.0	4×10^{-3}	6.0	8.4				

^aAverage crystallite dimension.

^bCalculated according to $S_{sp} = 3 \times 10^4 / (\rho \langle D \rangle)$, with ρ bulk density [13].

^cIn the total mass of the batch.

^dEstimated mass of the powder mechanically worked at each collision.

the subsequent spillover and diffusion into the Mg_2Ni intermetallic lattice [13]. It is therefore significant that the number of hydrogen atoms chemisorbed per second, $3.2 \times 10^{20} \text{ atoms} \cdot \text{s}^{-1}$, relates either to the surface Ni atoms in the batch (1.2×10^{20}) or to the total bulk atoms of the absorbing Mg_2Ni phase (3.9×10^{22}). 1.2×10^{20} was obtained by considering the surface Ni density ($1.54 \times 10^{19} \text{ atoms} \cdot \text{m}^{-2}$) [13] times the Ni surface area ($16.9 \text{ m}^2 \text{g}^{-1}$) times the Ni mass in the batch (0.44 g). The value 3.9×10^{22} was calculated, by multiplying the actual mass of Mg_2Ni in the vial, expressed in moles, to the Avogadro number. This result suggests that the maximum absorbing rate of the thermal process is determined by the whole accessibility of the Ni activation sites. Furthermore, in these initial steps, no hydride product layers exist yet, at the alloy inter-phase, limiting the hydrogen penetration in its host lattice. It gives an additional explanation of the initial maximum rate.

The hydriding rate decreases of two order of magnitude at the end-stage of the static process, and it appears that hydrogen diffusion has been reduced because of (i) a decreasing inner hydride-intermetallic interlayer (contracting core model [14]); and (ii) an increasing hydride layer over the Mg_2Ni surface, which must be crossed throughout for further growth.

It could be of interest now to compare these results with the hydriding behaviour under milling. Our aim is to highlight the mechanochemical effects due to the external energy pulses. We have the opportunity to relate the two processes either at the beginning of the absorption, by comparing to the initial rate in Curve 1 and Curve 2, or at the saturation limit of the static process, by evaluating the rate increase due to the sudden action of the mechanical treatment. It was conceived that differences in the absorbing rate were due to local strained or excited states and thereby to the chemisorbed molecules at the impact events. As noted above for the process onset, hydriding under milling begins with a rate of $8.2 \times 10^{-5} \text{ mole} \cdot \text{g}^{-1} \text{ s}^{-1}$, which gives a net mechanochemical gain of $4.6 \times 10^{-5} \text{ mole} \cdot \text{g}^{-1} \text{ s}^{-1}$, equivalent to $4.1 \times 10^{20} \text{ atoms} \cdot \text{s}^{-1}$, with respect to the rate observed in the static trial. Considering the impact frequency of 29 s^{-1} given above, we found $1.4 \times 10^{19} \text{ atoms} \cdot \text{hit}^{-1}$. For a consistent view of the process this quantity must now be related to Ni surface atoms present in the powder fraction mechanically worked at the impact. Considering an entrapped mass of about $1 \times 10^{-4} \text{ g}$, an usually accepted quantity for similar dynamic conditions and mechanical arrangement [15, 16], an amount of about 1.6×10^{15} Ni surface atoms was calculated (6.2×10^{16} are the bulk Ni atoms in the same impacted fraction of powder). Entrapped masses differing by one order of magnitude would not change the essential lines of our reasoning. Relating these two quantities, that is the hydrogen atoms absorbed per hit and the surface Ni atoms in the worked powder, the following emerges that the Ni landing area in the impacted mass remains in a excited state able to create an excess stock of chemisorbed molecules. If one also considers that 1.4×10^{17} atoms exist in the Mg_2Ni free surface (we are still considering the impacted pow-

der fraction) it also appears that the excess quantity of activated hydrogen atoms dissolves across the inter-phase boundaries without diffusion constrains. And it provides a local instantaneous view of the macroscopic process.

Focusing on Curve 1, dotted bar, the rate increase caused by the milling action corresponds to an excess number of 5.5×10^{16} atoms per hit. This quantity is lesser than the mechanochemical gain calculated at the process beginning, and the drop could be ascribed to a bulk diffusion controlled step, as in the case of the static process. However the disrupting action of the mechanical pulses creates new interphase boundaries in the whole impacted mass, making the residual hydrogen-free core of the Mg_2Ni particles more accessible for the hydrogen dissolution. It could explain the absolute rate increase caused by the mechanical treatment at the end of the static absorption stage.

From a mechanochemical point of view, at the beginning of the process the mechanical work done on the entrapped particles is totally expended in the activation of the hydrogen molecules, while an extra fragmentation work is also demanded in the advanced hydriding stages. It is reflected in the mechanochemical yield, which decreases from $0.12 \text{ mole} \cdot \text{kJ}^{-1}$ to $6.5 \times 10^{-4} \text{ mole} \cdot \text{kJ}^{-1}$ respectively.

Amorphous Zr-based powder provides a different example of kinetic behaviour as shown in Fig. 3 where Curves 1 and 2 refers to hydriding runs carried out at 0.05 and 0.09 $\text{W} \cdot \text{g}^{-1}$ respectively. Curve 3 refers to a nanostructured sample obtained by controlled crystallization under heating and tested at the same I_M of sample 2. Following the initial incubation period, the transformation rate increases progressively up to a steady trend, where reaches its maximum value, thereafter the reaction decelerates. Furthermore, hydriding induces the separation of two phases, the ZrH_2 compound and an amorphous Ni reach hydride. Demixing phenomena underline a further difference with respect to the previous Mg-based samples. One also notes that the length of incubation period and the hydriding rate strongly depends on the milling

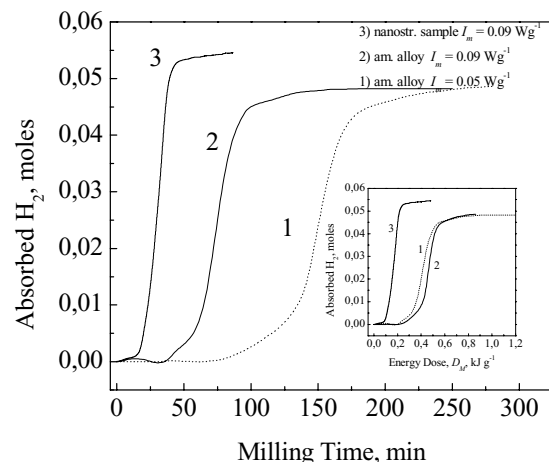


Figure 3 Absorption kinetic curves for amorphous and nanostructured $\text{Zr}_{55}\text{Cu}_{30}\text{Ni}_5\text{Al}_{10}$ powders obtained at the quoted milling intensity. Inset: the absorption curves are plotted against the energy dose, D_M .

intensity I_M , indicating that the hydrogen activation is really due to mechanochemical effects.

As above it is possible to define the dependence of the process on the surface character of the alloy by relating the transformation rate to either the bulk or surface atomic density of the impacted powder mass. At the maximum rate it was again found that the amount of the hydrogen uptake relates to the mass fraction worked out at the collision event. Complete results will be presented elsewhere. Here, we would like to draw attention on a special feature of the observed kinetic behaviour, which describes a further aspect of our methodological approach. The maximum hydriding rates increase with the milling intensity, however, in the case of the amorphous samples, the kinetic curves approach each other and the process become isokinetic as a function of the total energy dose D_M , as shown in the inset of Fig. 3. This result indicates that the same mechanical work must be done on the absorbing system to reach the same hydride fraction in the powder batch. The rate of the energy transfer speeds up the reaction, but does not modify the underlying mechanism of the hydriding reaction.

Conversely, a different path seems to rule the hydriding process in the case of the nanocrystalline sample for which a mechanochemical yield of 7.43×10^{-3} mole \cdot kJ $^{-1}$ was found, lesser than the one found for the Mg-based alloy at maximum transformation rate.

4. Conclusions

The detailed mechanism of gas absorption under milling has not as yet been deciphered, mostly because of the short lifetime of the non-equilibrium structures. It makes puzzling the conventional approaches to this topic. Our results, coupling structural and kinetic information with the characteristic parameters of the ball-vial dynamics, represent an initial attempt to approach on a quantitative basis the complex phenomenology of heterogeneous absorption under mechanical treatments. Along this line, the amount given here of the activated gas molecules as a function of local quantities (such as the surface or bulk density of the mass fraction

worked out at each impact), and further insights on the instantaneous transformation, albeit roughly estimated, provide an opportunity for absolute comparison on systems with quite different chemical, microstructural and thermodynamic features.

Acknowledgments

Prof. S. Enzo is gratefully acknowledged for useful advises and permanent support. G.C and L.S. thank MIUR-Rome for financial supports under PRIN contracts.

References

1. S. ORIMO, H. FUJII and T. YOSHINO, *J. Alloys Compd.* **217** (1995) 287.
2. L. ZALUSKI, A. ZALUSKA and J. O. STROM-OLSEN, *ibid.* **217** (1995) 245.
3. K. J. GROSS, P. SPATZ, A. ZUTTEL and L. SCHLAPBACH, *ibid.* **240** (1996) 206.
4. N. ISMAIL, M. UHLEMANN, A. GEBERT and J. ECKERT, *ibid.* **298** (2000) 146.
5. K. I. MOON and K. S. LEE, *ibid.* **264** (1998) 258.
6. W. RAJEWSKI, W. MAJCHRZYCHI and M. JURCZYK, *ibid.* **289** (1999) L6.
7. G. MULAS, S. SCUDINO and G. COCCO, *Mater. Sci. Eng. A*, in press.
8. Proceedings of the International Symposium on Metal Hydrogen Systems (MH2002), Annecy, September 2002, in press.
9. F. DELOGU, M. MONAGHEDDU, G. MULAS, L. SCHIFFINI and G. COCCO, *Int. J. Non-Equilibrium Proc.* **11** (2000) 235.
10. F. DELOGU, L. SCHIFFINI and G. COCCO, *Phil. Mag. A* **81** (2001) 1917.
11. P. Y. BUTYAGIN, *Sov. Sci. Rev. B Chem.* **14** (1989) 1.
12. L. LUTTEROTTI, R. CECCATO, R. DAL MASCHIO and E. PAGANI, *Mater. Sci. Forum* **278–281** (1998) 87.
13. J. R. ANDERSON, "Structure of Metallic Catalysts" (Academic Press, London, 1975).
14. MOSHE H. MINTZ and J. BLOCH, *Progr. Solid State Chem.* **16** (1985) 163.
15. J. S. BENJAMIN, *Mater. Sci. Forum* **88–90** (1992) 1.
16. G. COCCO, F. DELOGU and L. SCHIFFINI, *J. Mater. Synt. Process.* **8** (2000) 167.

Received 11 September 2003

and accepted 27 February 2004